Schweizerische Eidgenossenschaft
Confédération suisse
Confederazione Svizzera
Confederaziun svizra

Department of the Environment, Transport, Energy and Communication DETEC

Swiss Federal Office of Energy SFOE
Energy Research

Final report

ELYDEG

Degradation Signatures in Water Electrolyzers Operated with Variable Input

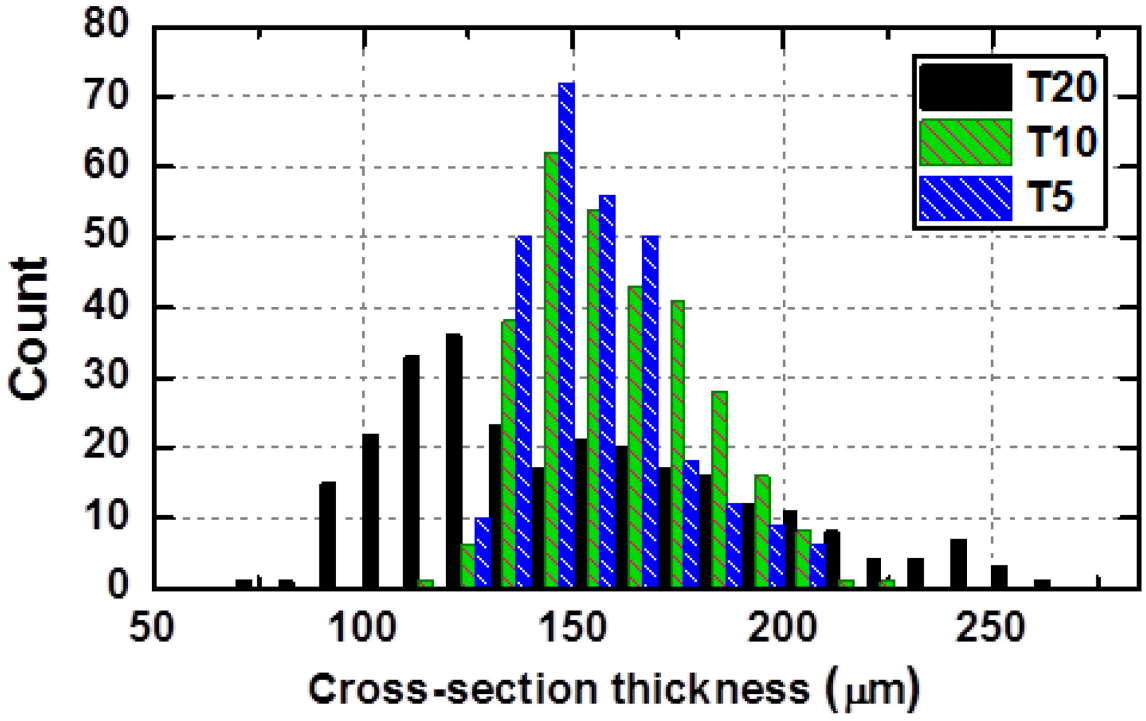

Date: 23 March 2018
Town: Villigen PSI

Publisher:
Swiss Federal Office of Energy SFOE
Research Programme Hydrogen and Fuel Cells
CH-3003 Bern
www.bfe.admin.ch

Agent:
Paul Scherrer Institut
Electrochemistry Laboratory
5232 Villigen PSI
www.psi.ch/lec

Author:
U. Babic, Paul Scherrer Institut, ugljesa.babic@psi.ch
L. Gubler, Paul Scherrer Institut, lorenz.gubler@psi.ch

SFOE head of domain: Stefan Oberholzer, stefan.oberholzer@bfe.admin.ch
SFOE programme manager: Stefan Oberholzer, stefan.oberholzer@bfe.admin.ch
SFOE contract number: SI/501198-01

Swiss Federal Office of Energy SFOE
Mühlestrasse 4, CH-3063 Ittigen; postal address: CH-3003 Bern
Phone +41 58 462 56 11 · Fax +41 58 463 25 00 · contact@bfe.admin.ch · www.bfe.admin.ch

Summary

Hydrogen generation through water electrolysis offers an interesting prospect to store excess electricity on the grid-scale in the context of future electricity supply scenarios with a large share of inherently intermittent renewable energy (wind, solar). This project was focused at understanding the implications and aging phenomena associated with the operation of a water electrolyzer under dynamic conditions, and addresses key materials issues, such as gas permeability and mechanical robustness of the electrolyte membrane.

A detailed analysis of efficiency loss contributions in the water electrolyzer cell necessitates the availability of relevant diagnostic tools. The ‘mass transport losses’ have so far included various contributions that were not further deconvoluted. We have introduced an analytic tool based on AC impedance spectroscopy used in fuel cells and adapted it to the electrolyzer cell to allow the quantification of proton transport losses in the catalyst layer of the oxygen electrode.

The main challenge towards understanding degradation mechanisms in a polymer electrolyte water electrolyzer (PEWE) is correlating degradation pathways with stressors (temperature, water impurities, high potential, etc.) and failure modes (performance and gas purity deterioration). We studied degradation using accelerated start-stop operation of the electrolyzer and saw more pronounced aging compared to state-state operation, which is of relevance for the dynamic operation of an electrolyzer.

Furthermore, the choice of porous transport layer material was shown to be crucial: the use of a soft carbon material on the hydrogen side (as in fuel cells) significantly reduces material creep, which is critical in particular with thin membrane materials. In this context, we evaluated in-house developed membranes and showed that they show very promising performance at much lower gas permeability. This is particularly important for the development of next generation water electrolyzers.

Project Overview & Key Results

The efficiency losses in a polymer electrolyte water electrolyzer (PEWE) cell can be extracted from the polarization curve according to the Tafel analysis shown in the previous work from the Electrochemistry Laboratory (1, 2), and are split into ohmic (η_{ohm}), kinetic (η_{act}), and mass-transport (η_{mtx}) contributions. The η_{ohm} is the result of the limited proton conductivity of the membrane and the contact resistances. The η_{act} is necessary for catalyzing the sluggish oxygen evolution reaction at the anode (the overpotential associated with the hydrogen evolution reaction can be neglected). The origin of the η_{mtx} is still not clear, and the findings in the literature are incoherent. Previous work has shown that η_{mtx} occurs on the anode side, and was hypothesized to stem from the two-phase flow through the anodic porous transport layer (PTLa) (2), and the removal of O_2 bubbles that hinder the water supply to the electrode (3). During this project we experimentally determined the overpotential related to the proton transport resistance in the catalyst layers. This overpotential has not been accounted for in PEWE and has so far been lumped together with general 'mass transport' losses.

The losses related to the catalyst layer play a significant role in fuel cell performance. To estimate their magnitude in PEWE, the experimental setup was modified to allow the controlled feed of N_2 to the anode cell compartment and the circulation of humid H_2 through the cathode cell compartment. The operation of the cell with the circulation of the aforementioned gases allowed us to probe the anode catalyst layer using impedance spectroscopy. The reactant for the anode reaction (in this case hydrogen oxidation reaction) is a result of hydrogen crossover from the cathode compartment, which eliminates any charge transfer reactions and other contributions to the measurement. The data was analyzed in accordance to the transmission line model, similar to the approach used in fuel cell catalyst characterization (4, 5). The equation for the impedance predicts a 45° slope at high frequencies, and a purely capacitive behavior at high frequencies, resulting in a vertical line in the Nyquist plot. If the impedance data fits the model (Figure 1a), the capacitive vertical projection corresponds to the proton resistance of the catalyst layer $R_{CLa}^{H+}/3$, which appears as a serial element in the polarization curve.

We have characterized the anode catalyst layers of Greenerity E400 catalyst coated membranes (CCMs) using titanium-sinter PTLs with different surface properties from GKN GmbH. The PTLs have designations T5, T10 and T20, corresponding to the nominal pore size. Previously, it has been demonstrated that the T10 was the optimum performing PTL for PEWE between the three. The impedance analysis showed $R_{CLa}^{H+}/3$ = 11.2 ± 1.8 mOhm cm^2 for the cell with the T10 PTLs, which is in line with the previous calculations on similar electrode types(6). Interestingly, the variation of PTLs resulted in different values for the $R_{CLa}^{H+}/3$ (Figure 1b), indicating that the PTL-induced structural inhomogeneity of the anode catalyst layer plays a role in the mass transport losses. These findings bring us closer to pinpointing the origin of the mass-transport losses, and demonstrate that the impedance characterization in H_2/N_2 operation is a powerful tool for optimizing and potentially diagnosing the degradation of catalyst layers.

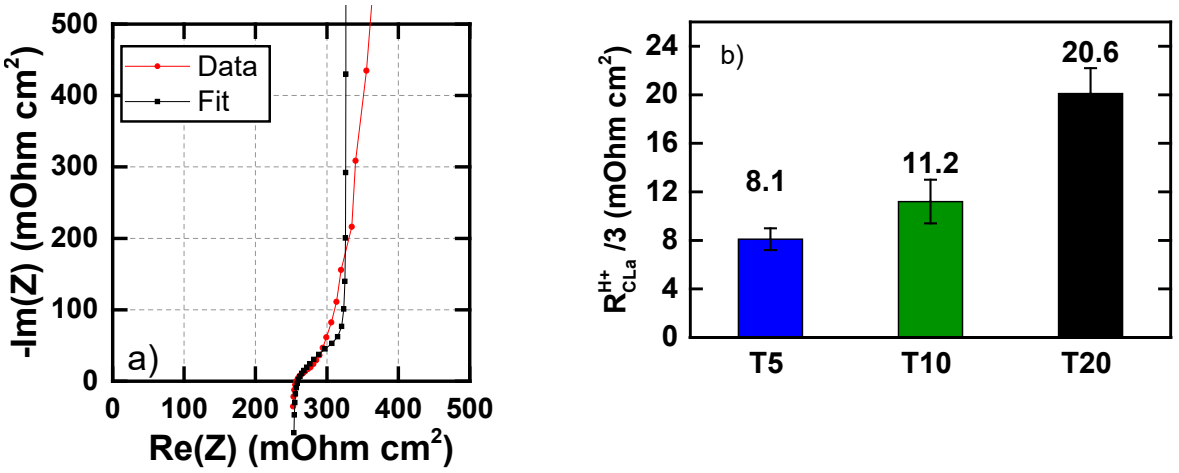

Figure 1. a) Impedance response of the CLa during the operation with H_2/N_2 at 60°C, and the fit according to the TLM. b) $R_{CLa}^{H+}/3$ extrapolated from the H_2/N_2 operation at 60°C for Greenerity CCMs assembled with T5/T10/T20 PTLs

In accordance to the project proposal, we have focused on specific degradation mechanisms and devised testing procedures to accelerate the degradation and increase material throughput. From the PTL variation it was evident that the coarse PTLs with large pore and particle sizes (e.g. T20 PTL) lead to pronounced creep of the CCM, whereas a fine PTL surface resulted in less pronounced CCM mechanical deformations. In order to mechanically stress the CCM and estimate the effects on the performance, a cell with T10 PTLs on both cathode and anode cell compartment was assembled (referred to as T10 cell from now on). The CCM is sandwiched between two rigid PTLs in this case, which under cell compression leads to pronounced creep. The other cell configuration was with a carbon based porous medium (Spectracarb 2050A + SGL 39BC) in the cathode cell compartment. The carbon fiber structure allows for the elastic deformation of the cathode PTL, which prevents mechanical creep of the CCM. This configuration will be referred to as 39BC. Two cells were operated in our in-house developed test benches at constant current density of 2 A/cm² and 60°C for 300 h. The electrolyzer test-stand had an ion exchange resin included in the anode recirculation loop to eliminate the contribution from the cation contamination from the metallic system components. Cell voltage and gas crossover were monitored during the electrolyzer operation. The beginning of test and end of test polarization curves were recorded with a potentiostat with an included impedance analyzer. The $R_{CLa}^{H+}/3$ were quantified as well using the previously described method.

The polarization curves recorded at the beginning and end of experiment (Figure 3a) show a significant loss of performance in the case of the T10 cell. The 39BC cell on the other hand shows improvement in the performance after 300 h of steady-state operation and an overall lower cell resistance after the experiment. The cell potential breakdown was done in accordance to the aforementioned Tafel analysis with the help of the high frequency resistance (HFR) obtained during the measurements. The results indicate the increase of all PEWE overpotentials. The increase of the η_{act} is related to the increased level of structural inhomogeneity in the anode catalyst layer due to the pronounced mechanical creep and deformation. Mechanical creep of the CCM implies in-plane cracks in the catalyst layer and the loss of contact to the PTL. These features are systematically evident in the post-test scanning electron microscopy analysis of the CCMs tested in the T10 configuration, whereas catalyst layers and the membrane-catalyst interface appear pristine in the case 39BC CCMs. Therefore the increased η_{ohm} most likely stems from the increased contact resistance in the case of T10 configuration. The most interesting is the difference in the η_{mtx} for the T10 cell before and after

300 h, which amounts up to ~50mV at 3 A/cm^2. This effect is not observed in the case of the 39BC cells. The effect can be explained by the increased proton transport resistance in the anode catalyst layer in the case of T10 cell (Figure 2b). The deformation of the electrode induces larger diffusion distances for the water, and an inhomogeneous water distribution in the catalyst layer. These deformations are present in a significantly smaller amount in the case of the 39BC cell, which is reflected in the $R_{CLa}^{H+}/3$ data.

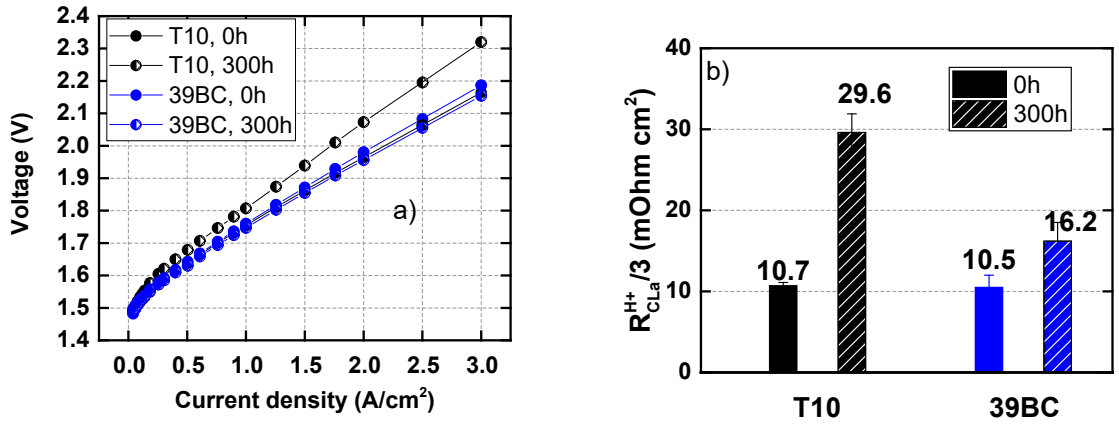

Figure 2. a) Polarization curves and b) $R_{CLa}^{H+}/3$ of the T10 and 39BC cells after conditioning and 300 h of steady-state operation at 2 A cm^{-2}, measured at 60°C

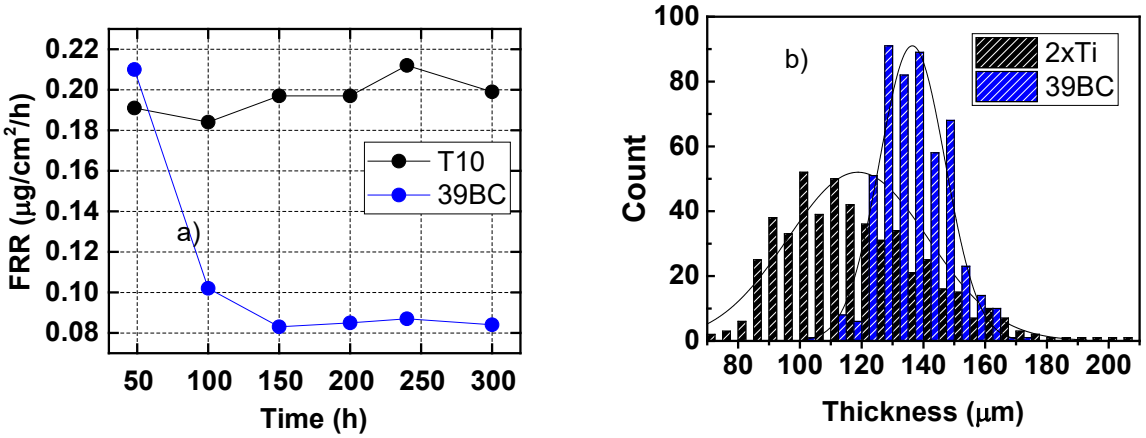

Figure 3. a) FRR during 300h of steady-state operation at 2 A cm^{-2} and 60°C for the T10 and 39BC cells. b) Thickness histogram of the CCMs from the T10 and 39BC cells, obtained by plotting measured CCM thickness from the SEM analysis.

Increased gas crossover has been shown to contribute to the chemical degradation of the polymer in fuel cells. Chemical degradation is estimated through the fluoride release rate measurements from the water from the cathode cell compartment. The hydrogen crossover in the case of the T10 cell was higher compared to the 39BC cell as a result of the CCM creep. During 300 h of operation, the cathode effluent water was collected for ion-chromatography analysis. The fluoride release rate was similar at the beginning of experiment for both cells, which is attributed to break-in effects. However, after 100 h the amount of fluoride in the water samples of the T10 cell was significantly higher (Figure 3a). This finding is important for the estimation of the CCM lifetime during prolonged exposure to chemical degradation stressors. It also demonstrates how the mechanical stressors such as cell

clamping force and the PTL surface morphology can accelerate the chemical decomposition of the membrane through increased gas crossover.

The cell in the 39BC configuration was operated in start-stop mode to accelerate the degradation of the anodic catalyst layer. It was found that the iridium catalyst surface is reduced during the off-state in the previous study from our laboratory. Formed surface hydroxide species have been correlated to higher activity, but compromised stability. We have varied the cell potential from 0 – 2 A/cm^2 in 30 s intervals for 250 h to stress this degradation mechanism. The CCM was analyzed in the SEM post-test, and the elemental mapping was done at 20 kV acceleration voltage to detect the precious metals that might have potentially dissolved and deposited in the membrane (Figure 4b). The precious metal (Ir+Pt) signal is plotted across the CCM thickness in the case of a CCM operated at start-stop conditions (Figure 2a, top) and a CCM operated at steady-state (Figure 4a, bottom). A diffuse iridium band in the vicinity of the anodic catalyst layer is detected in the case of a start-stop operated CCM, which does not occur as a result of steady-state operation.

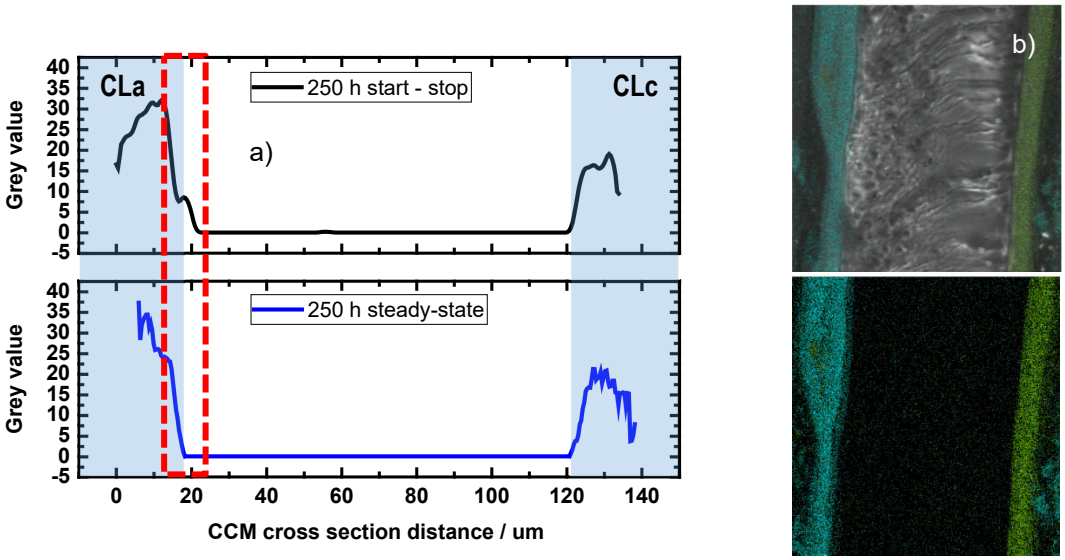

Figure 4. a) Ir-signal plot over the CCM cross-sections after 250 h of start-stop and steady-state operation, obtained from the SEM-EDX analysis, with the highlighted region near the CLa/PEM interface. b) SEM-EDX map of Ir (blue) and Pt (green) over the CCM cross-section.

The material modifications envisioned in the ELY-DEG project have been conducted in the framework of membrane synthesis and CCM characterization for the EU-NOVEL project. Novel membrane chemistries have been identified, with promising ion conductivity and gas barrier properties. The CCM fabrication was done by an external company for the reproducibility of results. The best performing PSI-CCM was based on the AMS-MGN chemistry (patent application in progress), outperforming the state-of-the-art Nafion based CCM with comparable thickness (Figure 4a). Moreover, the AMS-MGN CCM has displayed significantly better gas-barrier properties, resulting in a lower hydrogen crossover. The crosslinked variety (-DiPB) has even better gas barrier properties, and results in a cell performance that is on par with the 30 µm Nafion-based CCM.

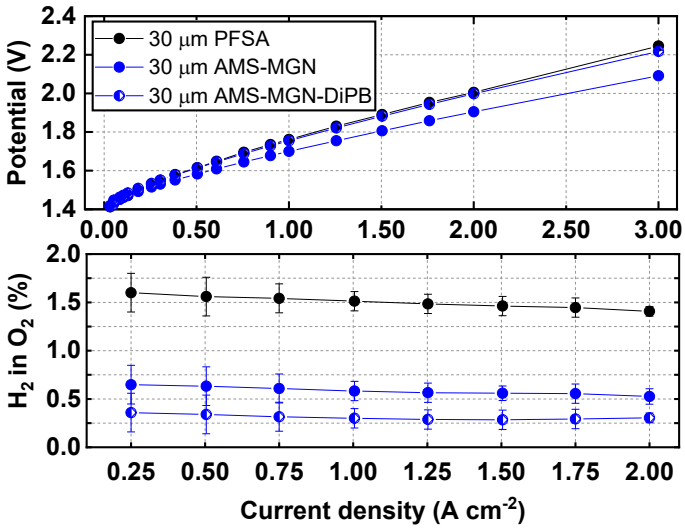

Figure 4. a) Polarization curves measured at 60°C and b) hydrogen in oxygen concentration for the 30µm Nafion-based and PSI-synthesized CCM

Outlook

Several publications are planned in the final year of the PhD student thesis, outlining the significant findings and diagnostics method employed during the thesis. Further experimental characterization of the in-house developed CCM will be conducted with the help of the newly acquired potentiostat with an impedance analyzer, and tailor made PTLs obtained in the cooperation with the German Aerospace Center (DLR). The ongoing collaboration with the Neutron Imaging group at the PSI is targeted at controlled operando contamination, and a joint beamline experiments are planned in 2018. In-addition, a master student project has been started in November 2017 with the goal of gas crossover suppression in thin membranes for PEWE. The findings in the framework of the thesis of Elisabeth Nilsson are relevant for the follow-up project ELY-TEMP, where crossover issues will be much more pronounced.

1. M. Suermann, T. J. Schmidt and F. N. Büchi, *Electrochimica Acta*, **211**, 989 (2016).
2. M. Suermann, K. Takanohashi, A. Lamibrac, T. J. Schmidt and F. N. Büchi, *Journal of The Electrochemical Society*, **164**, F973 (2017).
3. H. Ito, T. Maeda, A. Nakano, C. M. Hwang, M. Ishida, A. Kato and T. Yoshida, *International Journal of Hydrogen Energy*, **37**, 7418 (2012).
4. S. S. Kocha, in *Handbook of Fuel Cells*, John Wiley & Sons, Ltd (2010).
5. W. Gu, D. R. Baker, Y. Liu and H. A. Gasteiger, in *Handbook of Fuel Cells*, W. Vielstich, A. Lamm and H. A. Gasteiger (Editors), John Wiley & Sons, Ltd (2010).
6. M. Bernt and H. A. Gasteiger, *Journal of The Electrochemical Society*, **163**, F3179 (2016).